

We are IntechOpen, the world's leading publisher of Open Access books Built by scientists, for scientists

6,900

Open access books available

186,000

International authors and editors

200M

Downloads

Our authors are among the

154

Countries delivered to

TOP 1%

most cited scientists

12.2%

Contributors from top 500 universities



WEB OF SCIENCE™

Selection of our books indexed in the Book Citation Index
in Web of Science™ Core Collection (BKCI)

Interested in publishing with us?
Contact book.department@intechopen.com

Numbers displayed above are based on latest data collected.
For more information visit www.intechopen.com



Femtosecond Laser Pulses: Generation, Measurement and Propagation

Mounir Khelladi

Abstract

In this contribution some basic properties of femtosecond laser pulse are summarized. In sections 2.1–2.5 the generation of femtosecond laser pulses via mode locking is described in simple physical terms. In section 2.6 we deal with measurement of ultrashort laser pulses. The characterization of ultrashort pulses with respect to amplitude and phase is therefore based on optical correlation techniques that make of the short pulse itself. In section 3 we start with the linear properties of ultrashort light pulses. However, due to the large bandwidth, the linear dispersion is responsible for dramatic effects. To describe and manage such dispersion effects a mathematical description of an ultrashort laser pulse is given first before we continue with methods how to change the temporal shape via the frequency domain. The chapter ends with a paragraph of the wavelet representation of an ultrashort laser pulse.

Keywords: femtosecond laser pulse, ultrashort pulse, autocorrelation, characterization, dispersion, spectral phase, wavelet

1. Introduction

Propagation of ultrashort optical pulses in a linear optical medium consisting of free space [1–5], dispersive media [6, 7], diffractive optical elements [8–10], focusing elements [11] and apertures [12, 13] has been extensively studied analytically, though only a few isolated attempts have been made on numerical simulation. However, analytical methods have the limitations of not being able to handle arbitrary pulse profiles.

2. Ultrashort laser pulses generations

The central aim of this section is to give a concise introduction to nonlinear optics and to provide basic information about the most-widely used tunable femtosecond laser sources, in particular tunable Ti:sapphire oscillators and Ti:sapphire amplifiers or optical parametric amplifiers.

2.1 Titane sapphire oscillator

In 1982, the first Ti:sapphire laser was built by Mouton [14]. The laser tunes from 680 nm to 1130 nm, which is the widest tuning range of any laser of its class1.

Nowadays Ti:sapphire lasers usually deliver several watts of average output power and produce pulses as short as 6.5 fs (**Figure 1**) [14].

At high intensities, the refractive index depends nonlinearly on the propagating field. The lowest order of this dependence can be written as follows:

$$n(r) = n_0 + \frac{1}{2}n_2I(r) \tag{1}$$

n_0 : linear index refractive.

where n_2 is the nonlinear index coefficient and describes the strength of the coupling between the electric field and the refractive index n . The intensity is:

$$I(r) = e^{-gr^2} \tag{2}$$

The refractive index changes with intensity along the optical path and it is larger in the center than at the side of the nonlinear crystal. This leads to the beam self-focusing phenomenon, which is known as the Kerr lens effect (see **Figure 2**).

Consider now a seed beam with a Gaussian profile propagating through a nonlinear medium, e.g. a Ti:sapphire crystal, which is pumped by a cw radiation. For the stronger focused frequencies, the Kerr lens favors a higher amplification. Thus, the self-focusing of the seed beam can be used to suppress the cw operation, because the losses of the cw radiation are higher. Forcing all the modes to have equal phase (mode-locking) implies that all the waves of different frequencies will interfere (add) constructively at one point, resulting in a very intense, short light pulse.

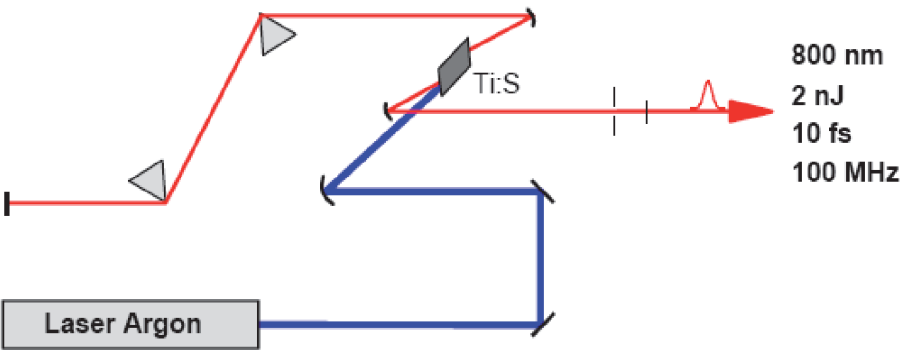


Figure 1.
A Ti: Sapphire oscillator.

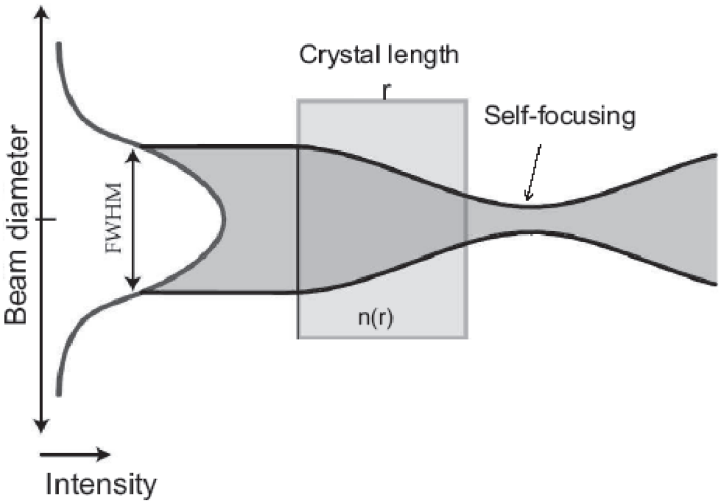


Figure 2.
The Kerr lens effect and self-focusing.

The pulsed operation is then favored, and it is said that the laser is mode-locked. Thus, the mode-locking occurs due to the Kerr lens effect induced in the nonlinear medium by the beam itself and the phenomenon is known as Kerr-lens mode-locking.

2.1.1 Examples



Auto TPL Tripler for laser oscillator.



Sprite XT: Tunable ultrafast Ti: sapphire laser (Figure 3).

The modes are separated in frequency by $\nu = c/2L$, L being the resonator length, which also gives the repetition rate of the mode-locked lasers:

$$\tau_{rep} = \frac{1}{T} = \frac{c}{2L} \tag{3}$$

Where L is length of cavity and T is period.

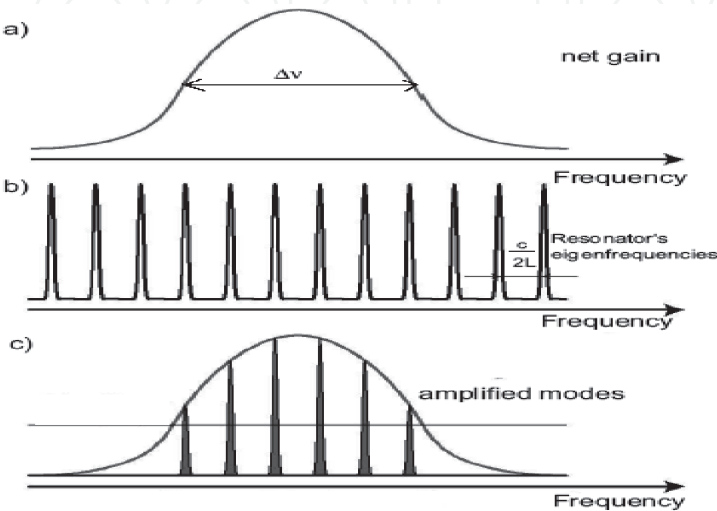


Figure 3. The Kerr lens mode-locking (KLM) principle. (a) the net gain curve (gain minus losses). In this example, from all the longitudinal modes in the resonator (b), only six (c) are forced to have an equal phase.

Moreover, the ratio of the resonator length to the pulse duration is a measure of the number of modes oscillating in phase. For example, if $L = 1\text{ m}$ and the emerging pulses have 100 fs time duration, there are 10^5 modes contributing to the pulse bandwidth. There are two ways of mode-locking a femtosecond laser: passive mode-locking and active mode-locking. In a laser cavity, these modes are equally spaced (with spacing depending on the cavity length). The electric field distribution with N such modes in phase (considered to be zero, for convenience) can be written as:

$$E(t) = \sum_n^{N-1} E_n e^{i\omega_0 + n\Delta\omega t} \propto \frac{e^{iN\Delta\omega t} - e^{i\omega_0 t}}{e^{i\Delta\omega t} - 1} \quad (4)$$

Where ω_0 is the central frequency and $\Delta\omega$ is the mode spacing, this appears as a carried wave with frequency domain.

n : is integer from 1 to N .

The laser intensity is given by

$$I(t) \propto [E(t)]^2 = \frac{\sin^2[(2n+1)\Delta\omega \cdot t/2]}{\sin^2(\Delta\omega \cdot t/2)} \quad (5)$$

Where $E(t)$: electrical field.

This is series of pulses with width inversely proportional to the number of modes that are locked in phase of the mode spacing. The concept of mode-locking is easier said than done.

Figure 4. shows how the time distribution of a laser output depends upon the phase relations between the modes. **Figure 4a** is the resultant intensity of two modes in phase **Figure 4b**, is the resultant intensity of five modes in phase and a period repetition of a wave packet from the resultant constructive interference can be seen.

2.2 CPA laser system

CPA is the abbreviation of chirped pulse amplification. Chirped pulse amplification is a technique to produce a strong and at the same time ultrashort pulse. The concept behind CPA is a scheme to increase the energy of an ultrashort pulse while avoiding very high peak power in the amplification process.

In the CPA technique, ultrashort pulses are generated typically at low energy $\sim 10^{-9}\text{ J}$, with a duration around 10^{-12} – 10^{-14} seconds and at a high repetition rate of about 10^8 1/s in an oscillator (**Figure 5**).

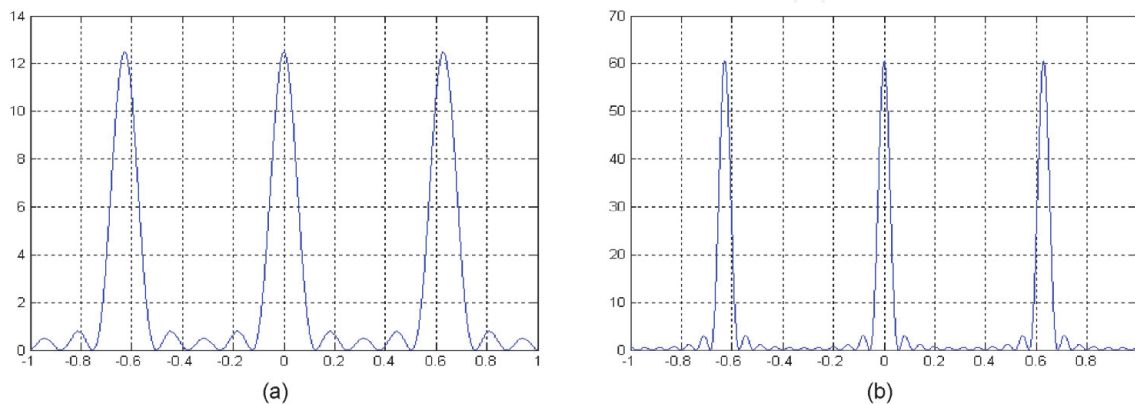


Figure 4.

The influence of the phase relation between oscillating modes on the output intensity of the oscillation. (a) Two modes in phase, and (b) five modes in phase.

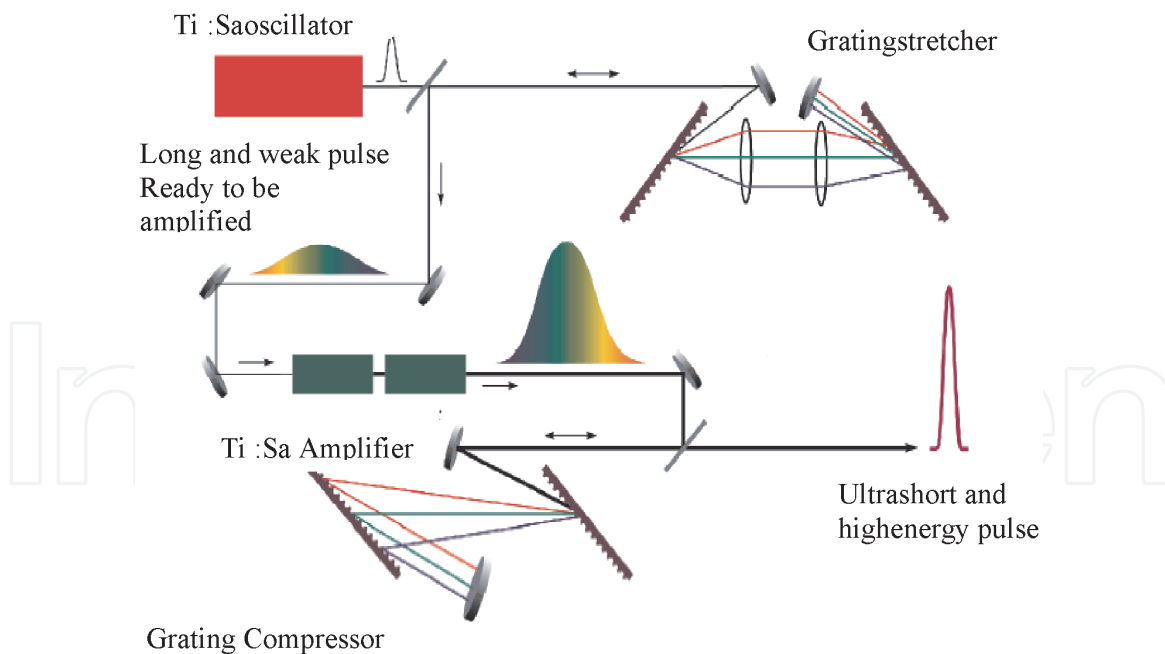


Figure 5.
 Schematics of a chirped pulse amplification system, showing the duration and energy level of the signal at the different stages of the system.

2.3 Multipass and regenerative amplification

Two of the most widely used techniques for amplification of femtosecond laser pulses are the multipass and the regenerative amplification. In the multipass amplification different passes are geometrically separated (see **Figure 6a**).

The regenerative amplification technique implies trapping of the pulse to be amplified in a laser cavity (see **Figure 2b**). Here the number of passes is not important. The pulse is kept in the resonator until all the energy stored in the amplification crystal is extracted. Trapping and dumping the pulse in and out of the resonator is done by using a Pockelcell (or pulse-picker) and a broad-band polarizer [15].

Of all potential amplifier media, titanium- doped sapphire has been the most wide spread used. It has several desirable characteristics which make it ideal as a high-power amplifier medium such as a very high damage threshold ($\sim 8\text{-}10\text{ J/cm}^2$), a high saturation fluence, and high thermal conductivity.

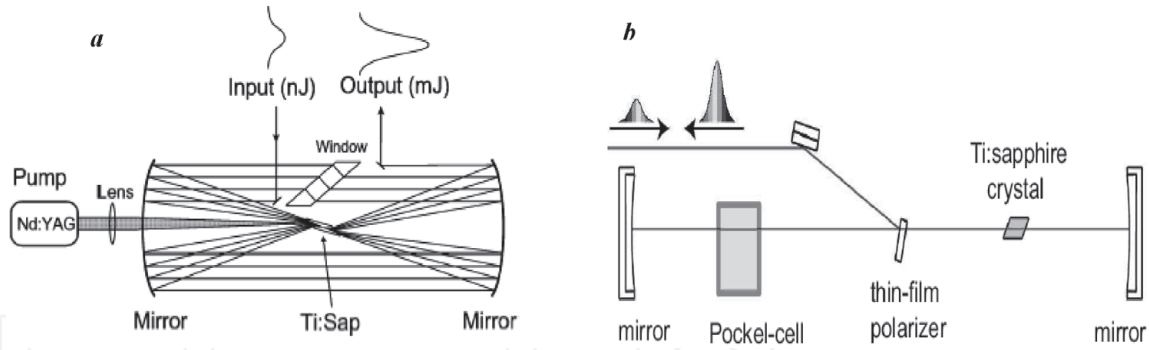
2.4 Stretcher-compressor

By using a dispersive line (combination of gratings and/or lenses), the individual frequencies within a femtosecond pulse can be separated (stretched) from each other in time (see **Figure 7a**).

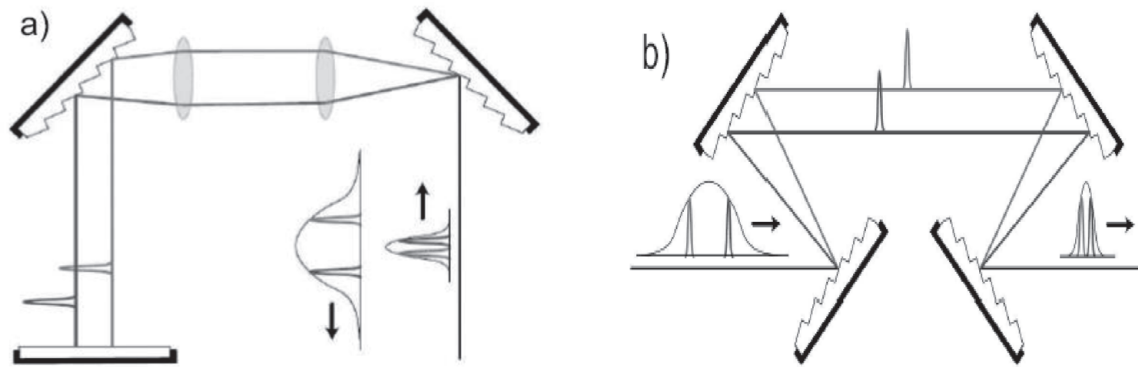
In normal materials, low frequency components travel faster than high frequency components; in other words, the velocities of large wavelength components are higher than that of shorter ones. These materials induce a positive group velocity dispersion on a propagating pulse. To compensate the positive GVD (Group Velocity Dispersion) and rephase the dephased components a setup which produces negative group velocity dispersion is needed [15].

2.4.1 Grating compressor

Four identical gratings in a sequence as shown in **Figure 8** make up a grating compressor. A pulse impinges on the first gratings with an angle of θ . Then from the second grating the spectral components in the spectrum travel together in parallel

**Figure 6.**

(a) The amplifier configuration uses two spherical mirrors in a multi-pass confocal configuration to make the signal pass eight times through the amplifying medium, (b) schematic principle of a regenerative amplifier.

**Figure 7.**

Principle of a stretcher (a) and a compressor (b). The stretcher setup extends the temporal duration of the femtosecond pulse, whereas the gratings' arrangement in the compressor will compress the time duration of the pulse. Both setups are used in femtosecond amplifiers.

directions but with wavelength dependent position (spatially chirped). The gratings are set in such a way that their wavelength dispersions are reversed which implies that the exiting ray from the second grating is parallel to the incident ray to the first grating.

The group delay induced by the grating compressor is given

$$T_g = \frac{2L}{c \cdot \sqrt{1 - \left(\frac{\lambda}{d} - \sin\gamma\right)^2}} \left[1 + \left(\frac{\lambda}{d} - \sin\gamma\right) \sin\gamma \right] \quad (6)$$

where, λ is the light wavelength, L is the distance between the gratings, d is the grating's constant and γ is the incidence angle of the beam to the first grating. Dispersion of the group delay is obtained as:

$$\text{GDD} = \frac{d^2 T_g}{d\omega^2} = -\frac{\lambda^3 L}{\pi c^2 d^2} \left[1 - \left(\frac{\lambda}{d} - \sin\gamma\right)^2 \right]^{-3/2} \quad (7)$$

GDD is Group Delay dispersion.

The third order dispersion produced in the grating compressor will be:

$$\text{TOD} = \frac{1}{L} \frac{d^3 T_g}{d\omega^3} = -\frac{d^2 T_g}{d\omega^2} \frac{6\pi\lambda}{c} \left[\frac{1 + \frac{\lambda}{d} \sin\gamma - \sin^2\gamma}{1 - \left(\frac{\lambda}{d} - \sin\gamma\right)^2} \right] \quad (8)$$

TOD is Third Order Dispersion.

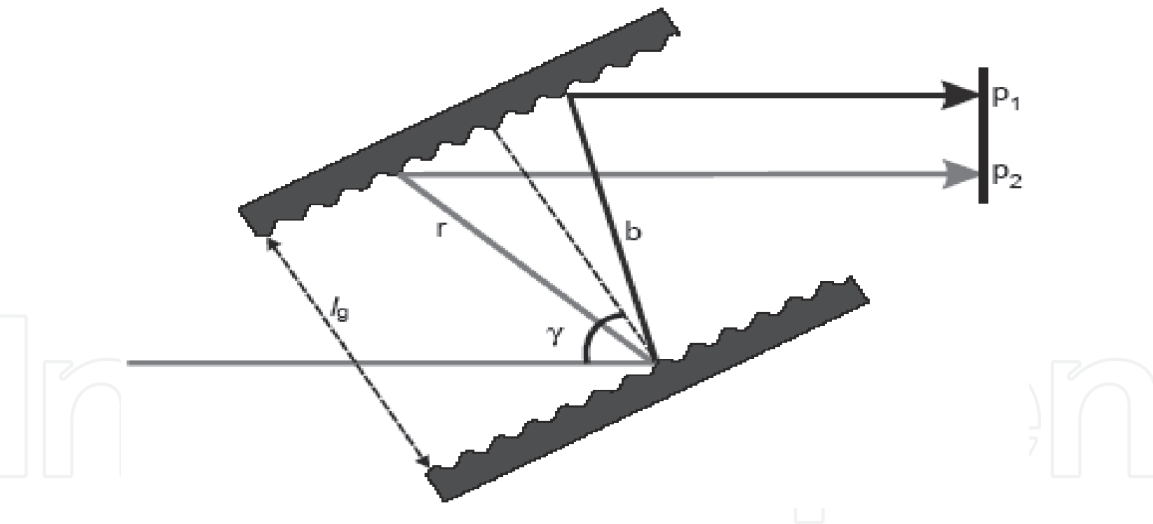


Figure 8. Grating pairs used in the control of dispersion. R and b indicate the relative paths of arbitrary long- and short-wavelength rays. γ is the (Brewster) angle of incidence at the prism face. Light is reflected in the plane (p_1 – p_2) in order to remove the spatial dispersion shown.

2.4.2 Prism compressor

A prism compressor is built of four sequentially arranged identical prisms used in a geometry similar to **Figure 9**; often at their minimum deviation (to decrease geometrical (spatial) distortion of prisms on the beam) and in their Brewster angle (to minimize power loss). Because of the symmetry in the arrangement, it is possible to place a mirror after the second prism (as we did in the grating compressor setup) perpendicular to the beam propagation direction. The first prism spreads the pulse spectral components out in space. In the second prism the red frequencies of the spectrum must pass through a longer length in the glass than the blue frequencies.

The optical path of a ray propagating in the compressor is defined as [15]: GDD will result

$$GDD = \frac{4L\lambda^3}{2\pi^2c^2} \left\{ \sin\beta \left[\frac{d^2n}{d\lambda^2} + \left(\frac{dn}{d\lambda} \right)^2 \left(2n - \frac{1}{n^3} \right) \right] - 2 \cos\beta \left(\frac{dn}{d\lambda} \right)^2 \right\} \quad (9)$$

β : is angle.

The third order dispersion can also be evaluated in the same manner to that used above

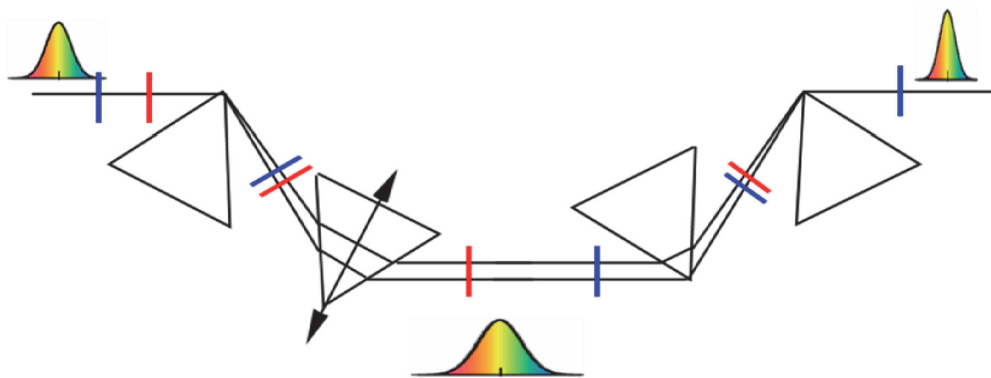


Figure 9. Pulse compressor.

$$TOD = -\frac{L^4}{4\pi^2 c^3 L} \left[3 \frac{d^2 n}{d\lambda^2} - \lambda \frac{d^3 n}{d\lambda^3} \right] \quad (10)$$

n : is refractive index.

2.5 Mathematical description of laser pulses

In order to understand the behavior of ultrashort light pulses in the temporal and spectral domain, it is necessary to formulate the relation between the two domains mathematically. It is important to introduce the concept of the amplitude and the phase of the electric field because the generation, measurement, and shaping of ultrashort laser pulses is based on measuring and influencing these properties. The electric field in the time-domain is invariably connected with its counterpart $E(w)$ in the frequency-domain via a Fourier transform:

2.5.1 Pulse duration and spectral width

The statistical definitions are usually used in theoretic calculations and given as

$$\langle t^2 \rangle = \frac{\int_{-\infty}^{+\infty} t^2 |E(t)|^2 dt}{\int_{-\infty}^{+\infty} |E(t)|^2 dt}; \quad \langle w^2 \rangle = \frac{\int_{-\infty}^{+\infty} w^2 |E(w)|^2 dw}{\int_{-\infty}^{+\infty} |E(w)|^2 dw} \quad (11)$$

In case of Gaussian pulse is easy to determine pulse duration and spectral width by applying FWHM (Full Width Half at Maximum) of intensity. One can show that these quantities are related through the following universal inequality.

$$\Delta w \Delta \tau \geq 1/2 \quad (12)$$

Therefore, one defines the pulse duration $\Delta \tau$ as the Full Width at Half Maximum (FWHM) of the intensity profile and the spectral width Δw as the FWHM of the spectral intensity. The Fourier inequality is then usually given by

$$\Delta w \Delta \tau \geq K \quad (13)$$

where K is a numerical constant, depending on the assumed shape of the pulse.

2.5.1.1 Gaussian pulse

The Gaussian pulse, which is most commonly used in ultrashort laser pulse characteristics. The pulse is linearly chirped and represented by

$$A(t) = A_0 \exp \left(\frac{-(1 + i\alpha)t^2}{\tau_g^2} \right) \text{ with } \Delta \tau_p = \sqrt{2 \ln 2} \tau_g \quad (14)$$

A_0 : amplitude, α : chirp,

τ_g : pulse duration at FWHM.

$\Delta \tau_p$: pulse duration at FWHM after propagation.

The instantaneous frequency is given as

$$\omega(t) = \omega_0 + \frac{d\phi(t)}{dt} = \omega_0 - \frac{2\alpha}{\tau_g^2}t \tag{15}$$

ω_0 : central pulsation.

$\omega(t)$: instantaneous pulse.

$\phi(t)$ is instantaneous phase.

The spectral intensity can be derived by taking the Fourier-transform of Eq.14, it also has the Gaussian shape [16].

The shortest possible pulse, for a given spectrum, is known as the *transform-limited pulse duration*. It should be noted that Eq. (13) is not equality, i.e. the product can very well exceed K . If the product exceeds K the pulse is no longer transform-limited and all frequency components that constitute the pulse do not coincide in time, i.e. the pulse exhibits frequency modulation is very often referred to as a *chirp* (**Figure 10**).

2.5.2 Time domain description

Since in this paper the main emphasis is on the temporal dependence, all spatial dependence is neglected, i.e., $E(x,y,z,t) = E(t)$. the electric field $E(t)$, is a real quantity and all measured quantities are real. However, the mathematical description is simplified if a complex representation is used:

$$\tilde{E}(t) = \tilde{A}(t).e^{-i\omega_0 t}. \tag{16}$$

where $\tilde{A}(t)$ is the complex envelope, usually chosen such that the real physical field is twice the real part of the complex field, and ω_0 is the carrier frequency, usually chosen to the center of the spectrum. In this way the rapidly varying is separated from the slowly varying envelope $\tilde{A}(t)$. $\tilde{E}(t)$ can be further decomposed into:

$$\tilde{E}(t) = |\tilde{E}(t)|.e^{i\phi_0}.e^{-i\phi(t)} = |\tilde{E}(t)|.e^{i\phi_0}.e^{-i(\phi(t)-\phi_0)}. \tag{17}$$

$\phi(t)$ is often to as the temporal phase of the pulse and ϕ_0 the absolute phase, which relates the position of the carrier wave to the temporal envelope of the pulse (see **Figure 11**). In $\phi(t)$ the strong linear term due to the carrier frequency, ωt , is omitted. which means that a nonlinear temporal phase yields a time-dependent frequency modulation- the pulse is said to carry a chirp (illustrated in **Figure 11b**).

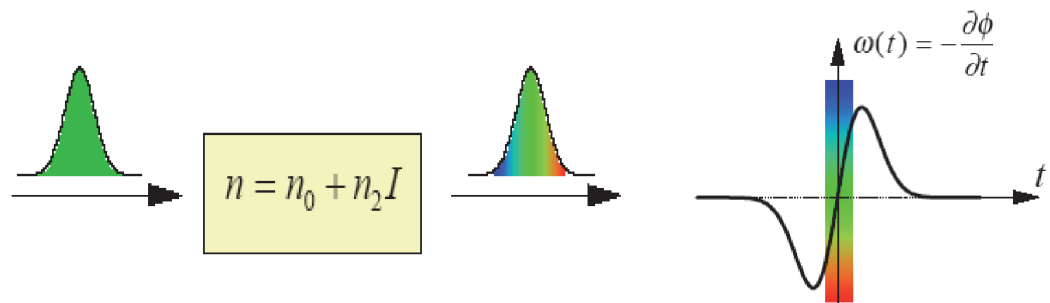


Figure 10. Self-phase modulation. Variation in the instantaneous frequency $\omega(t)$ of the transmitted pulse after the propagation through a nonlinear medium with a positive nonlinear index of refraction n_2 .

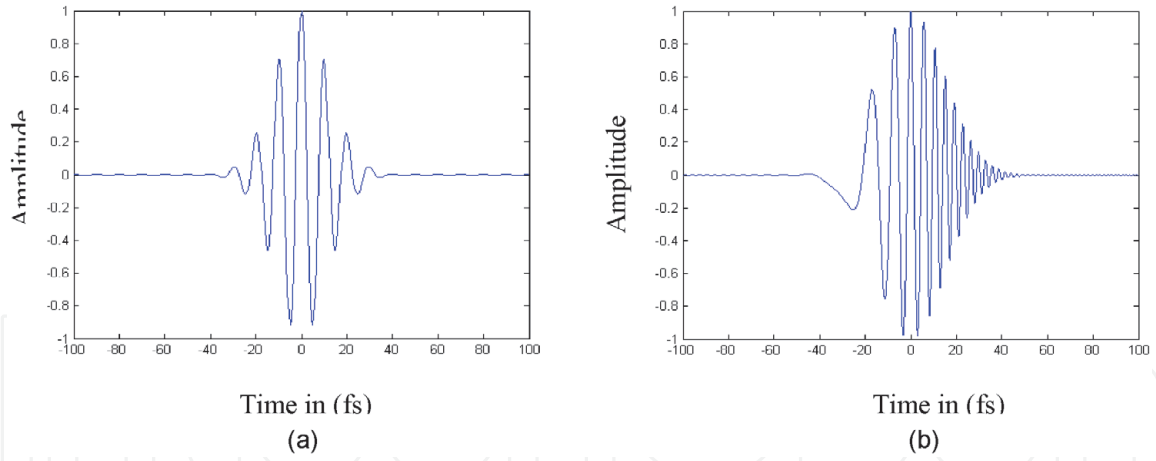


Figure 11.

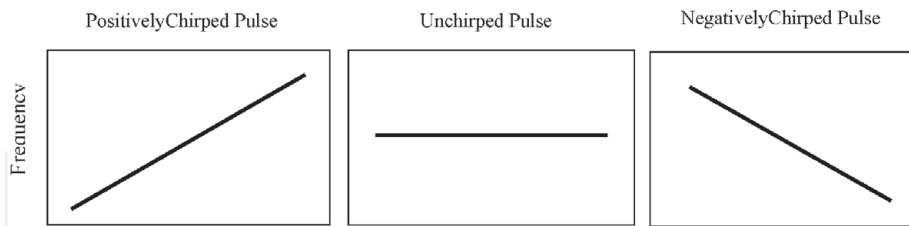
(a) The electric field of an ultra-short lasers pulse, (b) the electric field of an ultrashortlasers pulse with a strong positive chirp.

An ultrashort pulse of light will lengthen after it has passed through glass as the index of refraction, which dictates the speed of light in the material, depends nonlinearly on the wavelength of the light. The wavelength of an ultrashort pulse of light is formed from the distribution of wavelengths either side of the center wavelength with the width of this distribution inversely proportional to the pulse duration.

2.5.2.1 Phase and chirp

Instantaneous phase function of $E(t)$ can be described as the sum of temporal phase and product of carrier frequency with time by the relation $w(t) = \frac{d}{dt} \phi(t) + w_0 t$.

Carrier frequency w_0 has been chosen by minimizing of temporal variation of phase $\phi(t)$. The first derivation of $w(t)$ is defined by temporally-dependent carrier frequency as the result of applying the derivation we receive relation expended in series. Then carrier frequency time denotes quadratic chirp.



Positive chirp is when leading edge of pulse is red-shifted in relation to central wavelength and trailing edge is blue-shifted. Negative chirp happens in opposite case. Linear chirp, instantaneous frequency varies linearly with time. The presence of chirp results in significant different delays between the spectrally different components of laser pulse causing pulse broadening effect and leading to a duration-bandwidth.

Chirps always appear when ultrashort laser pulses propagate through a medium such as air or glass, where the spectral components of the pulse are subject to a different refractive index. This effect is called *Group Velocity Dispersion* (GVD).

2.5.3 Lens frequency domain description

The frequency representation is obtained from the time domain by a complex Fourier transform,

$$E(\omega) = \frac{1}{\sqrt{2\pi}} \int_{-\infty}^{+\infty} E(t) \cdot e^{-i\omega t} dt. \quad (18)$$

Just as in the time domain, $\tilde{E}(\omega)$ can be written as:

$$\tilde{E}(\omega) = |\tilde{E}(\omega)| e^{i\varphi(\omega)}. \quad (19)$$

where $\varphi(\omega)$ now denotes the spectral phase. An inverse transform leads back to the time domain,

$$\tilde{E}(t) = \frac{1}{\sqrt{2\pi}} \int_{-\infty}^{+\infty} \tilde{E}(\omega) \cdot e^{i\omega t} d\omega. \quad (20)$$

From Eq. (20) it is clear that $\tilde{E}(t)$ can be seen as a superposition of monochromatic waves. A common procedure is to employ Taylor expansion

$$\varphi(\omega) = \varphi_0 + \sum_{n=1}^{\infty} \frac{1}{n!} a_n (\omega - \omega_0)^n \text{ with } a_n = \left. \frac{d^n \varphi}{d\omega^n} \right|_{\omega=\omega_0}. \quad (21)$$

$\varphi(\omega)$ is spectral phase, ω is pulsation, and a_n is variation of the spectral phase with pulsation.

It can be seen by inserting this Taylor expansion into Eq. (21) that the first, two terms will not change the temporal profile of the pulse.

2.6 Ultrashort pulse measurement techniques

The most commonly used technique of ultrashort laser pulse width measurement is concerned with the study of the temporal intensity profile $I(t)$ through its second-order correlation function that is obtained by the second-harmonic generation. Ultrashort - pulse characterization techniques, such as the numerous variants of frequency resolved optical gating (FROG) and spectral phase interferometry for direct electric-field reconstruction (SPIDER), fail to fully determine the relative phases of wellseparated frequency components. If well-separated frequency components are also characterized gate pulses are used [17].

2.6.1 Non-interferometric techniques

2.6.1.1 Intensity autocorrelation

Complex electric field $E(t)$ corresponds to intensity $I(t) = |E(t)|^2$ and an intensityautocorrelation function is defined by

$$A(\tau) = \int_{-\infty}^{+\infty} I(t)I(t + \tau)dt \quad (22)$$

$A(\tau)$ is quadrature detection

$I(t)$ is intensity and $E(t)$ is electrical field

Two parallel beams with a variable delay are generated, then focused into a second-harmonic-generation crystal to obtain a signal proportional to $E(t) + E(t + \tau)$. Only the beam propagating on the optical axis, proportional to the cross

product $E(t)E(t - \tau)$ is retained. This signal is then recorded by a slow detector, which measures

$$I(\tau) = \int_{-\infty}^{+\infty} |E(t)E(t - \tau)|^2 dt = \int_{-\infty}^{+\infty} I(t)I(t - \tau) dt \quad (23)$$

$I(\tau)$ is exactly the intensity autocorrelation $A(\tau)$.

This numerical factor, which depends on the shape of the pulse, is sometimes called the deconvolution factor. If this factor is known, or assumed, the time duration (intensity width) of a pulse can be measured using an intensity autocorrelation. However, the phase cannot be measured [17, 18].

2.6.1.2 FROG

The technique of Frequency-Resolved Optical Gating (FROG) has been introduced by Trebino and coworkers. In FROG technique signal E_1 has been temporally shifted about τ through time-delay element in respect with signal E_2 . Then, two signals have been in nonlinear medium non-interferometrically overlapped. As the result of SFG or DFG process (at the efficient phase matching conversion) one receive the FROG signal.

In construction with process II also collinear geometry is possible.

$$E_{FROG}(\Omega, \tau) \propto \int_{-\infty}^{+\infty} E_1(t - \tau)E_2(t) \exp(i\Omega t) dt \quad (24)$$

$$\propto \int_{-\infty}^{+\infty} \tilde{E}_1(w)\tilde{E}_2(\Omega - w) \exp(iw\tau) dw \quad (25)$$

$$\propto \int_{-\infty}^{+\infty} dt \int_{-\infty}^{+\infty} \tilde{E}_1(w)E_2(t) \exp(-iwt) \exp(i\Omega t + iw\tau) dw \quad (26)$$

The spectral intensity

$$I_{FROG}(\Omega, \tau) \propto |E_{FROG}(\Omega, \tau)|^2 \quad (27)$$

Where:

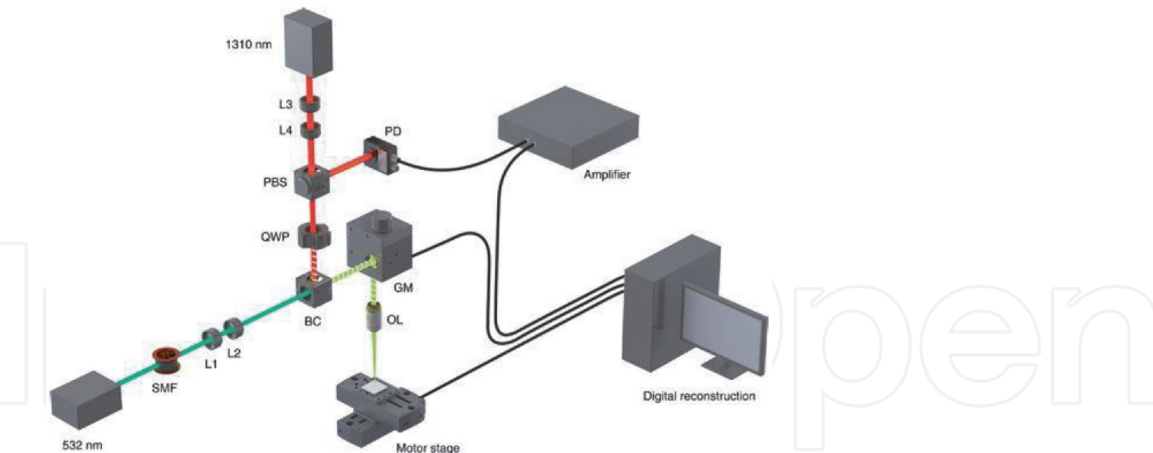
τ is delay between two temporal electrical field $E_1(t)$ and $E_2(t)$

Ω is delay between two spectral electrical field $E_1(w)$ and $E_2(w)$

$I_{FROG}(\Omega, \tau)$ is called FROG-trace. Relations (25), (26) are only the mathematical representation of Eq. (24). The task of receiving unknown complex signals E_1 and E_2 from measured FROG trace is known as the FROG reconstruction problem.

The resulting trace of intensity versus frequency and delay is related to the pulse's spectrogram, a visually intuitive transform containing both time and frequency information. Using phase retrieval concepts that the FROG trace yields the full intensity $I(t)$ and phase $\phi(t)$ of an arbitrary ultrashort pulse. As has been already mentioned, several schemes and methods exist for frequency-resolved optical gating as a technique for the full characterization of ultrashort optical signals as complex electric fields [14, 19].

2.6.1.2.1 Examples



Experimental setup. PARS microscopy with 532-nm excitation and 1310-nm integration beams. BC, beam combiner; GM, galvanometer mirror; L, lens; OL, objective lens; PBS, polarized beam splitter; PD, photodiode; QWP, quarter wave plate; SMF, single mode fiber.

2.6.2 Interferometric techniques

2.6.2.1 Interferometric autocorrelation

Setup for an interferometric autocorrelator is similar to the field autocorrelator above, with the following optics added: L: converging lens, SHG: secondharmonic generation crystal, F: spectral filter to block the fundamental wavelength. A nonlinear crystal can be used to generate the second harmonic at the output of a Michelson interferometer in a collinear geometry. In this case, the signal recorded by a slow detector (**Figure 12**).

$$I(\tau) = \int_{-\infty}^{+\infty} |E(t) + E(t - \tau)|^2 dt \tag{28}$$

$I(\tau)$ is called the interferometric autocorrelation. It contains some information about the phase of the pulse: the fringes in the autocorrelation trace wash out as the spectral phase becomes more complex (**Figure 13**).

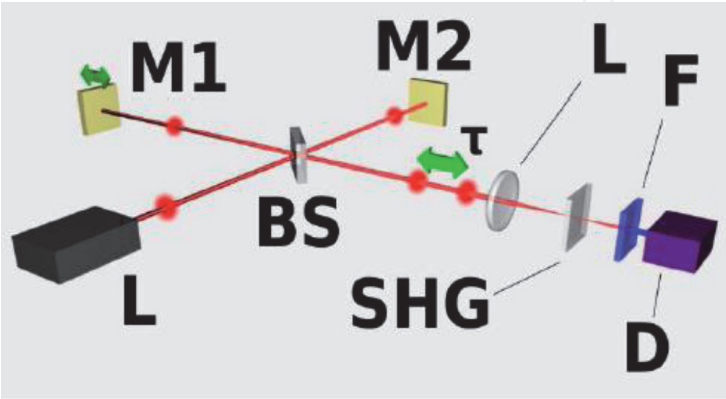


Figure 12. Setup for an interferometric autocorrelator, similar to the field autocorrelator above, with the following optics added: L: Converging lens, SHG: Second-harmonicgeneration crystal, F: Spectral filter to block the fundamental wavelength.

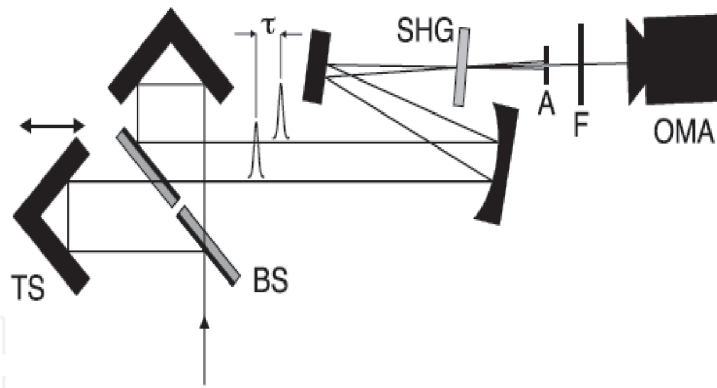


Figure 13.

FROG reconstruction scheme. When both E_1 and E_2 have been unknown, then we deal with blind-FROG problem. When $E_1 = E_2$ then we have to do with SHG-FROG problem.

2.6.2.2 Spider

The Spectral Phase Interferometry for Direct Electric-field Reconstruction technique (SPIDER) is based on spectral interferometry and needs no components which has to be shifted over the measurement process. From the signal $E(t)$ that should be characterized, the copy-signal is being generated by beam splitter

$$E(t - \tau) \exp[i\omega_0 \tau] \quad (29)$$

The time between the signal and copy itself has been established through fixed position at the optical delay-line. Then the copy of signal goes through phase filter (dispersive medium, for instance SF10 glass), so arises the signal

$$E_M(t) = F^{-1}\{\tilde{E}(w) \exp[i\varnothing_M(w)]\} \quad (30)$$

E_M electrical field at point M

\varnothing_M : phase of electrical field

Through the phase filter electric field $\tilde{E}(w)$ get additional spectral phase $\varnothing_M(w)$, which corresponds to temporal extension $E(t)$. From the signals

$$E_M(t) \text{ and } E(t - \tau) \exp[i\omega_0 \tau] + E(t) \quad (31)$$

SFG-Signal can be created

$$E_{SFG}(t) \propto E_M(t) \{E(t - \tau) \exp[i\omega_0 \tau] + E(t)\} \quad (32)$$

$$= E_M(t)E(t - \tau) \exp[i\omega_0 \tau] + E_M(t)E(t) \quad (33)$$

As square law detectors are not sensitive to the phase, the measurement of the intensity (whether it is spatial or spectral) is an easy task but the measurement of the phase needs indirect solutions (**Figure 14**).

Spectral interferometry allows us obtain difference between two spectral phases. To the spectral interferometry spectrum, one should apply fast Fourier transform and as the product one will achieve in form of one center peak and two sidebands lower peaks in the time domain (**Figure 15**).

Centered peak contains only spectrum information. One filter out two peaks and from existing one can receive spectral phase difference by applied inverse fast Fourier transform. To the main advantages of the SPIDER method can be counted following properties: pulse retrieval is direct (non-iterative), minimal data are required: only one spectrum yields spectral phase [20].

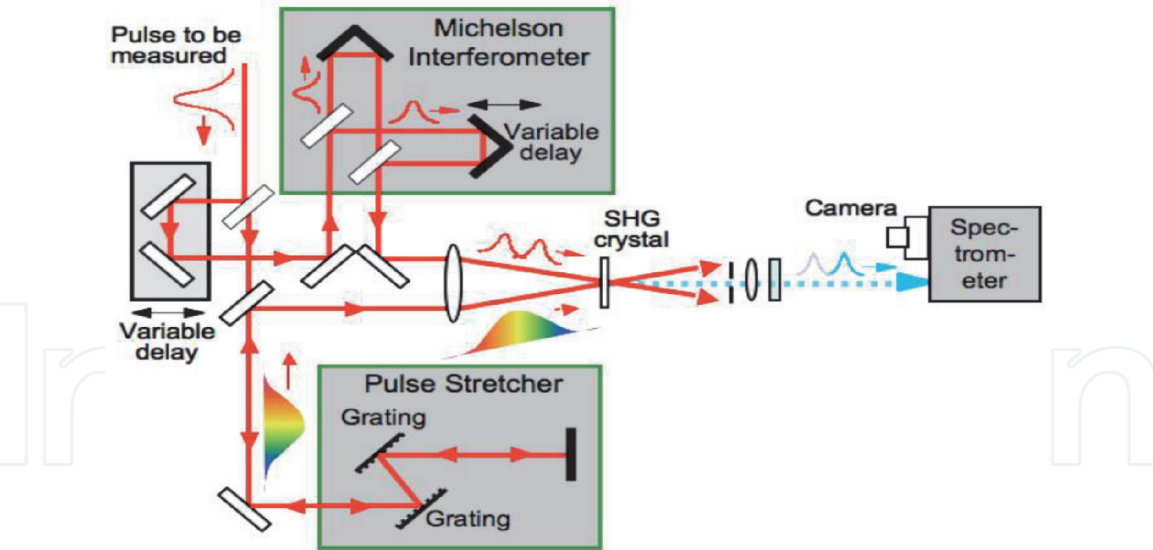


Figure 14.
Main steps of SPIDER technique.

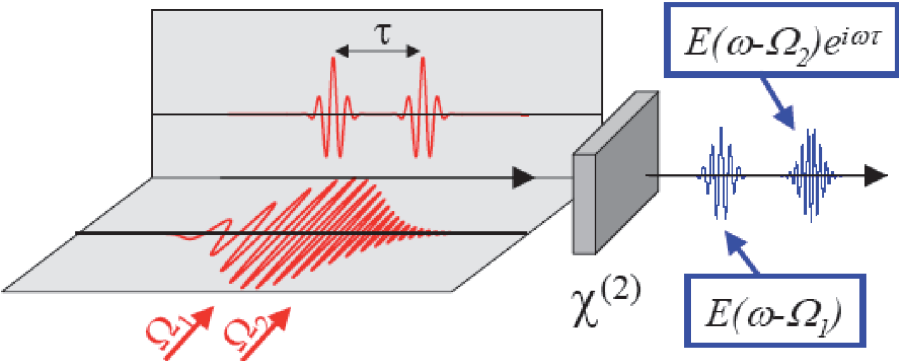
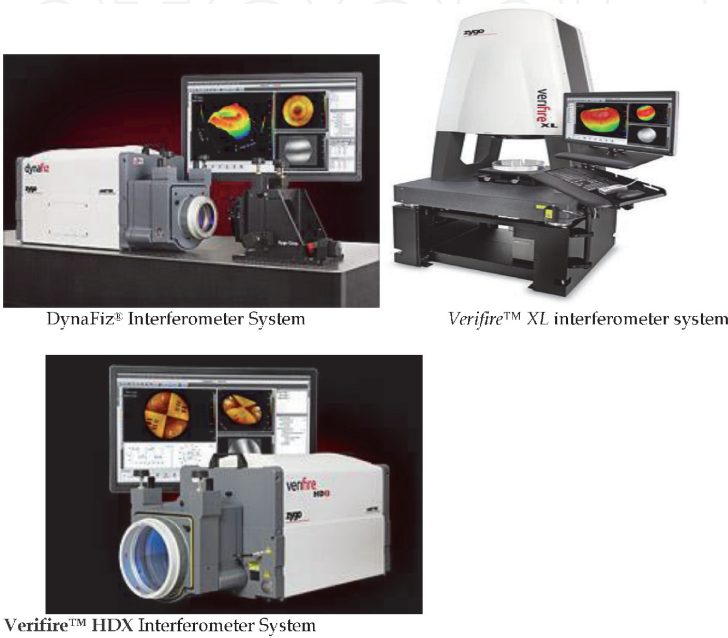


Figure 15.
Generation of two sheared replicas of the input pulse by non-linear interaction with a chirped pulse.

2.6.2.2.1 Examples



3. Propagation of a light pulse in a transparent medium

The frequency Fourier transform of a Gaussian pulse has already been given as

$$E(w) = \exp\left(\frac{-(w - w_0)^2}{4\Gamma}\right). \quad (34)$$

$\Gamma = \frac{2\log 2}{\Delta_0^2}$ is coefficient of function Gaussian

An ultrashort Fourier limited pulse has a broad spectrum and no chirp; when it propagates a distance through a transparent medium, the medium introduces a dispersion to the pulse inducing an increase in the pulse duration. To investigate and determine the dispersion, we assume a Gaussian shape for the pulse. The electric field of the pulse is given as Eq. (35).

After the pulse has propagated a distance z , its spectrum is modified to

$$E(w, z) = E(w) \exp[\pm ik(w)z], k(w) = \frac{n(w).w}{c}, \quad (35)$$

where $k(w)$ is now a frequency-dependent propagation factor. In order to allow for a partial analytical calculation of the propagation effects, the propagation factor is rewritten using a Taylor expansion as a function of the angular frequency, assuming that $\Delta w \ll w_0$ (this condition is only weakly true for the shortest pulses). Applying the Taylor expansion to Eq. (37), the pulse spectrum becomes.

Δw is bandwidth of the pulse and w_0 is central pulsation

$$k(w) = k(w_0) + k'(w - w_0) + \frac{1}{2}k''(w - w_0)^2 + \dots, \quad (36)$$

where $k' = \left(\frac{dk(w)}{dw}\right)_{w_0}$ and $k'' = \left(\frac{d^2k(w)}{dw^2}\right)_{w_0}$,

$$E(w, z) = \exp\left[-ik(w_0)z - ik'(w - w_0)z - \left(\frac{1}{4\Gamma} + \frac{i}{2}k''\right)(w - w_0)^2\right]. \quad (37)$$

The time evolution of the electric field in the pulse is then derived from the calculation of the inverse Fourier transform of Eq. (39),

$$e(t, z) = \int_{-\infty}^{+\infty} E(w, z).e^{-iwt}dw \quad (38)$$

so that

$$e(t, z) = \sqrt{\frac{\Gamma(z)}{\pi}}. \exp\left[iw_0\left(t - \frac{z}{V_\phi(w_0)}\right)\right] \times \exp\left[-\Gamma(z)\left(t - \frac{z}{V_g(w_0)}\right)^2\right] \quad (39)$$

Where

$$V_\phi(w_0) = \left(\frac{w}{k}\right)_{w_0}, V_g(w_0) = \left(\frac{dw}{dk}\right)_{w_0}, 1/(\Gamma(z)) = 1/\Gamma + 2ik''z. \quad (40)$$

In the first exponential term of Eq. 40, it can be observed that the phase of the central frequency w_0 is delayed by an amount $\frac{z}{V_\phi}$ after propagation over a distance z . Because the phase is not a measurable quantity, this effect has no observable

consequence. The phase velocity $V_{\phi}(w_0)$ measures the propagation speed of the plane wave components of the pulse in the medium. These plane waves do not carry any information, because of their infinite duration.

The second term in Eq. 40 shows that, after propagation over a distance z , the pulse keeps a Gaussian envelope. This envelope is delayed by an amount z/V_g , V_g being the group velocity. The second term in Eq. 40 also shows that the pulse envelope is distorted during its propagation because its form factor $\Gamma(z)$, defined as

Depends on the angular frequency w through $k''(w)$,

$$k'' = \left(\frac{d^2 k}{dw^2} \right)_{w_0} = \frac{d}{dw} \left(\frac{1}{V_g} \right)_{w_0}. \tag{41}$$

This term is called the “Group Velocity Dispersion”. The temporal width of the pulse at point z :

$$\Delta\tau_z = \Delta\tau_0 \sqrt{1 + 4.(\Gamma.k''z)^2}. \tag{42}$$

with $k'' = \frac{\lambda^3}{2.\pi.c^2} \frac{d^2 n}{d\lambda^2} \Gamma = \frac{2 \log 2}{\Delta_0^2}$,
 $\Delta\tau_0$ initial pulse before propagation inside the medium

3.1 Application in litharge index SF56 medium

In optical materials, the refractive index is frequency dependent. This dependence can be calculated for a given material using a Sellmeier equation, typically of the form

$$n^2(w) = 1 + \sum_{i=1}^m \frac{B_i w_i^2}{w_i^2 - w^2} \tag{43}$$

B_i is the coefficients of glass see in **Table 1**
The index of litharge SF56 is given by the following expression (43):

where w_i is the frequency of resonance and B_i is the amplitude of resonance. In the case of optical fibers, the parameters w_i and B_i are obtained experimentally by fitting the measured dispersion curves to Eq. (44) with $m = 3$ and depend on the core constituents [21].

3.2 Parameter of dispersion

An ultrashort Fourier limited pulse has a broad spectrum and no chirp; when it propagates a distance through a transparent medium, the medium introduces dispersion to the pulse inducing an increase in the pulse duration. We consider dispersions of orders two. The pulse broadens on propagation because of group velocity dispersion (GVD).

In summary, the propagation of a short optical pulse through transparent medium results in a delay of the pulse, a duration broadening and a frequency chirp. All these phenomena are increase with distance of propagation. We shown in

B_i	1.81651732	0.428893631	1.07186278
$\lambda_i(\mu m)$	0.0143704198	0.0592801172	121.419942

Table 1.
Parameters for litharge SF56 glasses.

Figure 16 that the duration broadening is not linear for ultrashort pulse. Specially under 70 fs or less. The Eq. (43) is not applicable for pulse less than 70 fs. For minimize these parameters we introduce the nonlinear phenomena as Self phase modulation (SPM), Soliton pulse, dispersion compensate fiber.

3.3 Group velocity dispersion

The Group Velocity Dispersion (GVD) is defined as the propagation of different frequency components at different speeds through a dispersive medium. This is due to the wavelength-dependent index of refraction of the dispersive material [22].

$$\varphi(w) = \varphi(w_0) + (w - w_0) \left. \frac{d\varphi}{dw} \right|_{w=w_0} + \frac{1}{2!} (w - w_0)^2 \left. \frac{d^2\varphi}{dw^2} \right|_{w=w_0} + \dots + \frac{1}{n!} (w - w_0)^n \left. \frac{d^n\varphi}{dw^n} \right|_{w=\Omega} \quad (44)$$

$$\left\{ \begin{array}{l} \varphi(\lambda) = \frac{2\pi}{\lambda} n(\lambda) z \\ \frac{d\lambda}{dw} = -\frac{\lambda^2}{2\pi c} \\ \frac{d\varphi}{dw} = -\frac{z}{c} \left[\frac{dn}{d\lambda} - n \right] \\ \frac{d^2\varphi}{dw^2} = +\frac{\lambda^3}{4\pi^3 c^2} \frac{d^2 n}{d\lambda^2} z \\ \frac{d^3\varphi}{dw^3} = -\frac{\lambda^4}{4\pi^2 c^3} \left[3 \frac{d^2 n}{d\lambda^2} + \lambda \frac{d^3 n}{d\lambda^3} \right] z \\ \frac{d^4\varphi}{dw^4} = +\frac{\lambda^5}{8\pi^3 c^4} \left[12 \frac{d^2 n}{d\lambda^2} + 8\lambda \frac{d^3 n}{d\lambda^3} + \lambda^2 \frac{d^4 n}{d\lambda^4} \right] z \\ \frac{d^5\varphi}{dw^5} = -\frac{\lambda^6}{16\pi^4 c^5} \left[60 \frac{d^2 n}{d\lambda^2} + 60\lambda \frac{d^3 n}{d\lambda^3} + 15\lambda^2 \frac{d^4 n}{d\lambda^4} + \lambda^3 \frac{d^5 n}{d\lambda^5} \right] z \\ \frac{d^6\varphi}{dw^6} = +\frac{\lambda^7}{32\pi^5 c^6} \left[360 \frac{d^2 n}{d\lambda^2} + 480\lambda \frac{d^3 n}{d\lambda^3} + 180\lambda^2 \frac{d^4 n}{d\lambda^4} + 24\lambda^3 \frac{d^5 n}{d\lambda^5} + \lambda^4 \frac{d^6 n}{d\lambda^6} \right] z \end{array} \right. \quad (45)$$

It seemsto methatwe can write $\phi^{(i)} = \frac{d^i \phi}{dw^i}$ as a recurrence, giving $\phi^{(i)}$ based on derivatives of order i , the index of refraction. Matrix form, we can write it

$$\begin{bmatrix} \phi^{(2)} \\ \phi^{(3)} \\ \phi^{(4)} \\ \phi^{(5)} \\ \phi^{(6)} \end{bmatrix} = (-1)^n 2\pi z \left[\frac{\lambda}{2\pi c} \right]^n \begin{bmatrix} 1 & 0 & 0 & 0 & 0 \\ 3 & 1 & 0 & 0 & 0 \\ 12 & 8 & 1 & 0 & 0 \\ 60 & 60 & 15 & 1 & 0 \\ 360 & 480 & 180 & 24 & 1 \end{bmatrix} \quad (46)$$

The various terms of the Taylor expansion to order n can be written in the shape of a matrix $[A]$, which's we can express various terms A_{ij} .

$$\phi(w) = \phi(w_0) + (w - w_0) \phi^{(1)} + \sum_{i=2}^p \frac{1}{i!} (w - w_0)^i \phi^{(i)} \Big|_{w=w_0}. \quad (47)$$

$\phi(w)$ is Taylor series of phase and $\phi^{(p)}$ is the orders of Taylor series

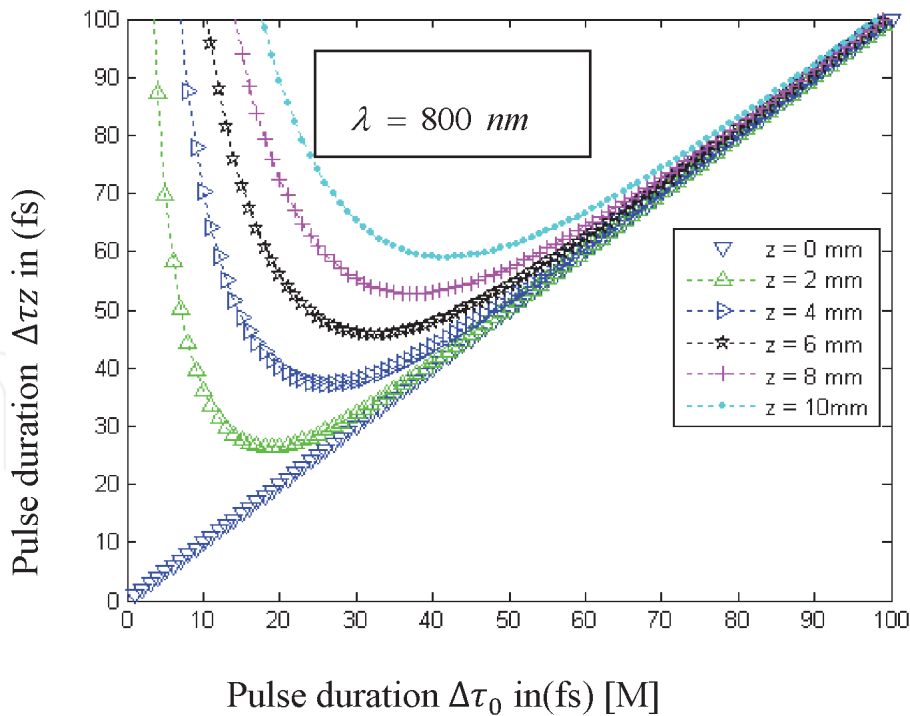


Figure 16.
 Temporal broadening of the transform- limited pulse for different values of the propagation distance z .

$$\varnothing^{(p)} = (-1)^p . 2\pi . z \left[\frac{\lambda}{2 . \pi . c} \right]^p \sum_{j=2}^p \lambda^{j-1} A(p-1, j-1) n^{(j)} \text{ with } p > 2 \tag{48}$$

Analytically known and experimentally observed propagation affects such as spectral shift, pulse broadening and asymmetry in dispersive media can be easily brought out in the simulation using formalism presented here. In addition, such studies can be extended to pulses of arbitrary temporal shape without any further algorithmic complexity by numerical simulation. Higher order dispersion effects can be handled easily in the numerical simulation unlike in the case of analytical calculation (**Figure 17**) [22].

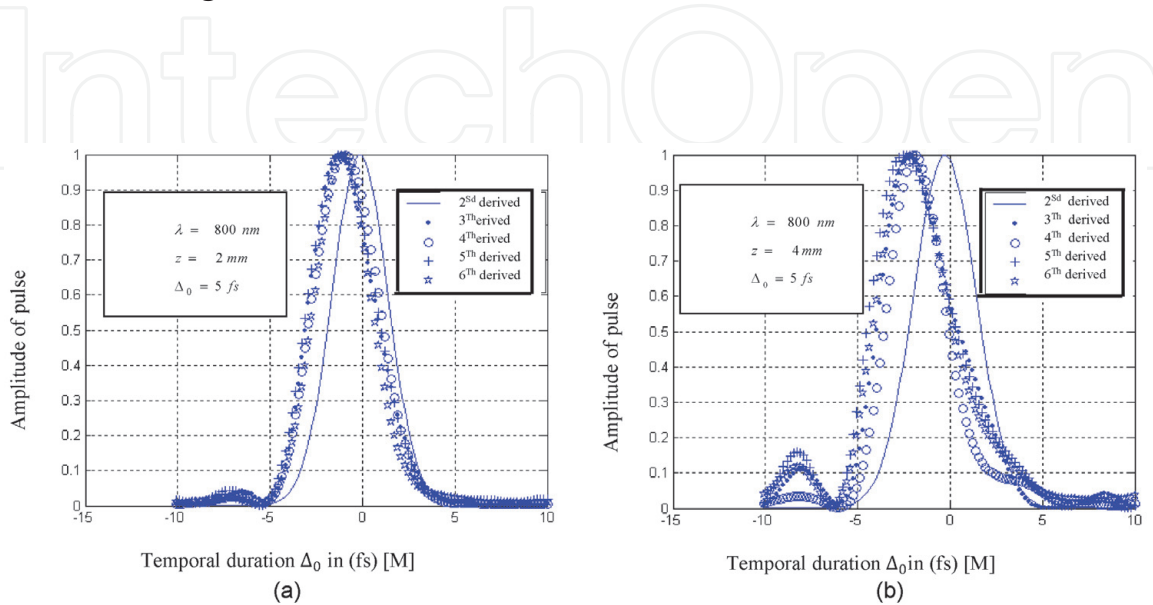


Figure 17.
 (a) The pulse broadens on propagation as a result of group velocity dispersion (GVD) (b) the pulse shape is no longer Gaussian, and it becomes asymmetric due to higher order dispersions.

4. Time-frequency decomposition

4.1 Wavelet theory

The wavelets are very particular elementary functions, these are the shortest vibrations and most elementary that one can consider. One can say that the wavelet east carries out a zooming on any interesting phenomenon of the signal which place on a small scale in the vicinity of the point considered [23].

4.2 Wavelet techniques

Starting with a signal $e(t)$, in plane $z = 0$, we define wavelet centered at Ω by (Figure 18):

$$\theta(\Omega) = E(w) \cdot \exp \left[-\frac{(w - \Omega)^2}{4\gamma} \right], \text{ with } E(w) = \frac{E_0}{2\pi} \sqrt{\frac{\pi}{\Gamma}} \exp \left[-\frac{(w - w_0)^2}{4\Gamma} \right], \quad (49)$$

$$\theta(t, z = 0) = TF\{\theta(\Omega, z = 0)\} \quad (50)$$

TF it is the Fourier Transform equation
z is the distance of propagation

$$\theta(t, z = 0) = E_0 \sqrt{\frac{\gamma}{\gamma + \Gamma}} \cdot \exp \left[-\frac{(w_0 - \Omega)^2}{4(\gamma + \Gamma)} \right] \cdot \exp \left[-\frac{\gamma\Gamma}{\gamma + \Gamma} t^2 \right] \cdot \exp \left[j \frac{\gamma w_0 + \Gamma\Omega}{\gamma + \Gamma} t \right] \quad (51)$$

- In time, the pulse is also Gaussian, of parameter $\frac{\gamma\Gamma}{\gamma + \Gamma}$.
- The maximum of amplitude of the wavelet $\theta(t, z = 0)$ vary with Ω , center frequency of analysis on Gaussian of parameter $\gamma + \Gamma$.
- The signal propagates in the positive z direction in a linear dispersive and transparent medium, which fills the half space $z > 0$ and whose refractive index is $n(w)$. After propagation, the wavelet $\theta(\Omega, x)$ may be written as

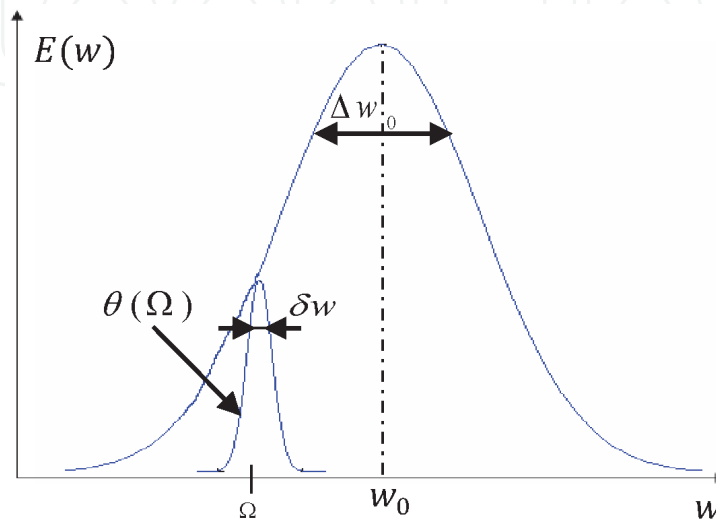


Figure 18.

Gaussian envelope decomposed on a number of wavelets calculates the electric field associated with the wavelet $\theta(\Omega, z = 0)$.

$$\theta(\Omega,z) = \frac{E_0}{2.\sqrt{\pi}\gamma}E(w).exp\left[-\frac{(w-\Omega)^2}{4\gamma}\right].exp\left[j\phi(w)\right]. \tag{52}$$

As already mentioned, $\tau_{wavelet}$ is large enough to ensure that analyzing function has only non negligible values over a spectral range lying in the neighborhood of Ω in (Figure 19). Under these circumstances, we have

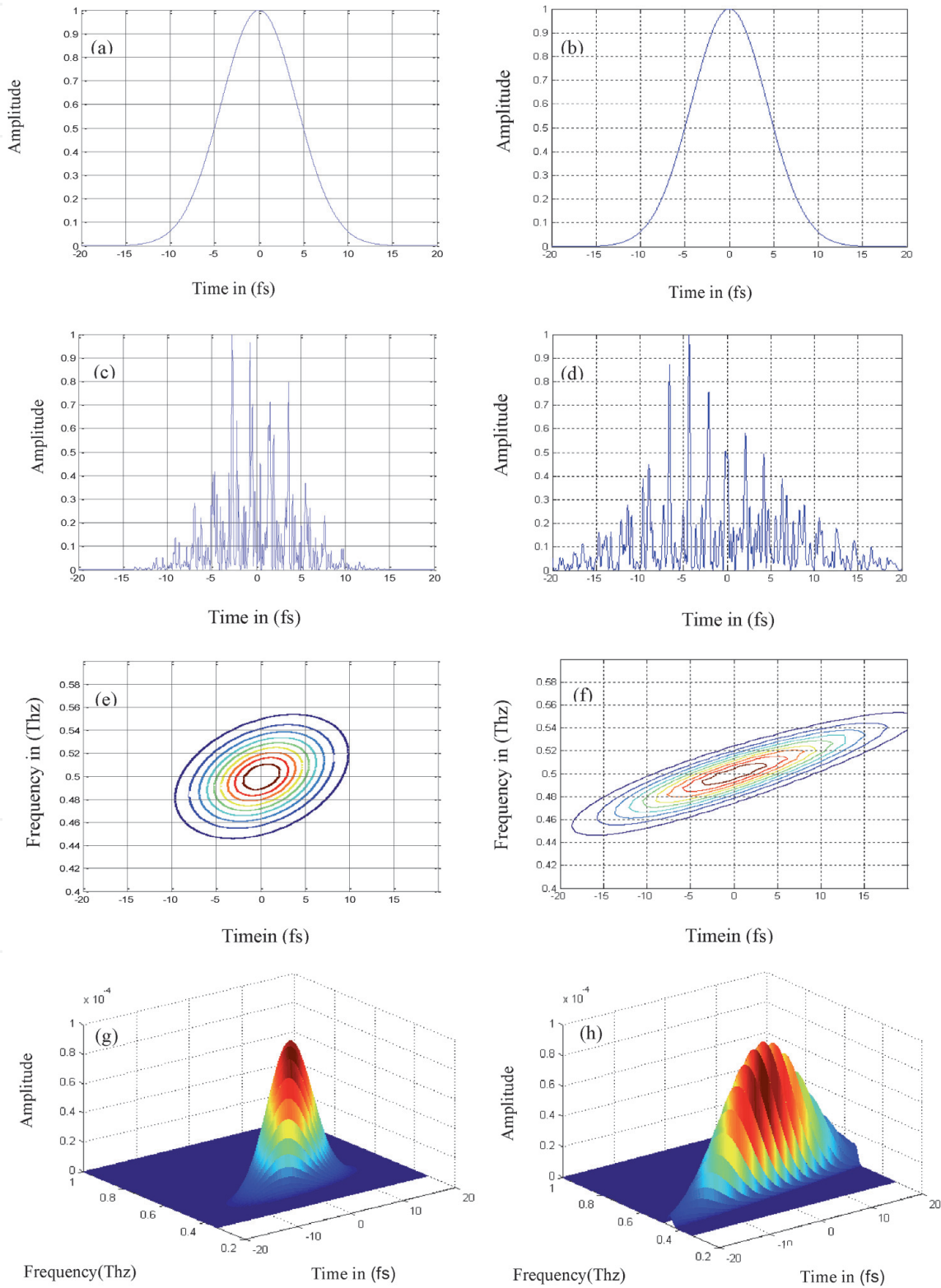


Figure 19. (a) Initial pulse, (c) pulse after propagation of the 10 cm in glass SF56 (e) contour of the wavelet, (g) the wavelet representation, (b) initial pulse, (d) pulse after propagation of the 10 cm in the silica medium, (f) contour of the wavelet, (h) the wavelet representation [22].

$$\begin{aligned} \varnothing(w) = \varnothing(\Omega) + (w - \Omega) \frac{d\varnothing}{dw} \Big|_{w=\Omega} + \frac{1}{2!} (w - \Omega)^2 \frac{d^2\varnothing}{dw^2} \Big|_{w=\Omega} + \dots + \frac{1}{n!} (w - \Omega)^n \frac{d^n\varnothing}{dw^n} \Big|_{w=\Omega} \\ + \theta(w)_{w=\Omega} \end{aligned} \quad (53)$$

Neglecting the higher terms in Eq. (49):

$$\varnothing(w) = \varnothing(\Omega) + (w - \Omega) \frac{d\varnothing}{dw} \Big|_{w=\Omega} + \frac{1}{2!} (w - \Omega)^2 \frac{d^2\varnothing}{dw^2} \Big|_{w=\Omega} + \theta(w). \quad (54)$$

$$\begin{aligned} \theta(\Omega, z) = \frac{E_0}{2\sqrt{\pi}\gamma} \sqrt{\frac{\pi}{\Gamma}} \exp \left[-\frac{(w - w_0)^2}{4\Gamma} \right] \\ \cdot \exp \left[-\frac{(w - \Omega)^2}{4\gamma} \right] \cdot \exp \left[j\varnothing^{(0)} + j(w - \Omega)\varnothing^{(1)} + \frac{1}{2}j(w - \Omega)^2 \cdot \varnothing^{(2)} \right] \end{aligned} \quad (55)$$

$$\theta(t, z) = \frac{1}{2\pi} \int_{-\infty}^{+\infty} \theta(\Omega, z) \cdot \exp(j\omega t) d\omega \quad (56)$$

We calculate the temporal electric field associated with the wavelet $\theta(\Omega, z)$.

$$\begin{aligned} \theta(t, z) = \frac{1}{2\pi} \frac{E_0}{2\sqrt{\pi}\gamma} \sqrt{\frac{\pi}{\Gamma}} e^{\left[-\frac{(\Omega - w_0)^2}{4\Gamma} \right]} e^{j\varnothing^{(0)}} \times e^{-\left[\frac{1}{4\Gamma} + \frac{1}{4\gamma} - \frac{1}{2}j\varnothing^{(2)} \right] \Omega^2} \cdot e^{\left[\frac{(\Omega - w_0)}{2\Gamma} - j\varnothing^{(1)} \right] \Omega} \\ \times \left(\int_{-\infty}^{+\infty} e^{-\left[\frac{1}{4\Gamma} + \frac{1}{4\gamma} - \frac{1}{2}j\varnothing^{(2)} \right] w^2} \cdot e^{\left[\frac{1}{4\Gamma} + \frac{1}{4\gamma} - \frac{1}{2}j\varnothing^{(2)} \right] 2\Omega w} \times e^{\left[-\frac{(\Omega - w_0)}{2\Gamma} - j\varnothing^{(1)} \right]} \cdot e^{j\omega t} dw \right) \end{aligned} \quad (57)$$

The amplitude of the incident Ω wavelet is given from Eq. (58) by

$$\begin{aligned} \theta(t, z) = \frac{E_0}{2\sqrt{\pi}\gamma} \sqrt{\frac{\Gamma(z)}{\Gamma}} \cdot \exp \left(j\varnothing^{(0)} \right) \exp \left(-\Gamma(z) \left[t + \frac{z}{V_g(\Omega)} \right]^2 \right) \\ \times \exp \left(-\frac{(\Omega - w_0)^2}{4\Gamma} \left[1 - \frac{\Gamma(z)}{\Gamma} \right] \right) \cdot \exp \left[j \left(1 - \frac{\Gamma(z)}{\Gamma} \right) \Omega + \frac{\Gamma(z)}{\Gamma} w_0 \right] \left(t + \frac{z}{V_g(\Omega)} \right). \end{aligned} \quad (58)$$

This wavelet is characterized by a Gaussian envelope. This decomposition is valid only for the values of Δw much larger than δw ($\Delta w \gg \delta w$).

The delay of group of the wavelet $\left[t + \frac{z}{V_g(\Omega)} \right]$ is characterized by a Gaussian envelope which is the temporal width.

The delay of group of the wavelet is inversely proportional to the velocity of group its envelope propagates without deformation [22].

4.3 Simulations

4.3.1 Parameters of the simulations

Pulse initial: $\Delta\tau_0 = 20 \text{ fs}$
(Wavelength) $\lambda = 800 \text{ nm}$

Pulse of the wavelet: $\Delta\tau_{\text{wavelet}} = 1000 \text{ fs}$

Longer of the medium: $z = 10 \text{ cm}$

To describe the propagation of the pulse, we only consider the propagation of the maximum of each wavelet in a three dimensional representation:

Figure 19(c) shows that when pulse propagate inside SF56 glass present minor dispersion and distortion compared to the silica fiber in **Figure 19d**.

Figure 19(e) shows that the SF56 glass resist in temporal domain than silica fiber as shown in **Figure 19(f)**. but, in frequency domain the both SF 56 glass and silica fiber are the same modification.

Figure 19(g) and **(h)** shown the amplitude of the wavelet

5. Conclusion

Generating ultrashort light pulses requires a laser to operate in a particular regime, called mode-locking which many be illustrated either in the frequency or the time domain. Depending on the particular case, one description is much more intuitive than the other and we have chosen to present the simpler approach. The generation of femtosecond laser pulses via mode locking is described in simple physical terms. As femtosecond laser pulses can be generated directly from a wide variety of lasers with wavelengths ranging from the ultraviolet to the infrared no attempt is made to cover different technical approaches.

The ability to accurately measure ultrashort laser pulses is essential to creating, using, and improving them, but the technology for their measurement has consistently lagged behind that for their generation. The result has been a long and sometimes quite painful history of attempts—and failures—to measure these exotic and ephemeral events. The reason is that many pulse-measurement techniques have suffered from, and continue to suffer from, a wide range of complications, including the presence of ambiguities, insufficient temporal and/or spectral resolution and/or range, an inherent inability to measure the complete pulse intensity and/or phase, an inability to measure complex pulses, and misleading results due to the loss of information due to idiosyncrasies of the technique or multishot averages over different pulses.

Finally, we have demonstrated here the possible decomposition of an ultrashort pulse into an infinite number of longer Fourier transform limited wavelets which propagate without any deformation through a dispersive medium. After propagation through the medium, the pulse may be visualized in a three-dimensional representation by the locus of the wavelet maxima.


Author details

Mounir Khelladi

Abou-bekrBelkaid University of the Tlemcen, Algeria

*Address all correspondence to: mo.khelladi@gmail.com

IntechOpen

© 2021 The Author(s). Licensee IntechOpen. This chapter is distributed under the terms of the Creative Commons Attribution License (<http://creativecommons.org/licenses/by/3.0>), which permits unrestricted use, distribution, and reproduction in any medium, provided the original work is properly cited. 

References

- [1] Florența A.C, Dynamics of Ultra-short Laser Pulse Interaction with Solids at the Origin of Nanoscale Surface Modification” geboren am 16.11.1971 in Berca, Rumänien Cottbus (2006)
- [2] Chritov, I.P., Propagation of femtosecond light pulses, *Opt. Commun.* 53, 364–366.
- [3] Sheppard, C.R, Xianosong, G, Free-space propagation of femtosecond light pulses, *Opt. Commun.* 133, 1–6. (1997)
- [4] Agrawal, G.P, Spectrum-induced changes in diffraction of pulsed beams, *Opt. Commun.* 157, 52–56. (1998).
- [5] Kaplan, A.E., Diffraction-induced transformation of near cycle and subcycle pulses, *J. Opt. Soc. Am. B* 15, 951–956. (1998)
- [6] Agrawal, G.P, Far-Field diffraction of pulsed optical beams in dispersive media, *Opt. Commun.* 167, 15–22. (1999).
- [7] Porras, M.A, Propagation of single-cycle pulse light beams in dispersive media, *Phys. Rev. A* 60, 5069–5073. (1998).
- [8] Ichikawa, H, Analysis of femtosecond-order optical pulses diffracted by periodic structure, *J. Opt. Soc. Am. A* 16, 299–304. (1999).
- [9] Pietstun, R., Miller, D.B., Spatiotemporal control of ultrashort optical pulses by refractive-diffractive-dispersive structured optical elements, *Opt. Lett.* 26, 1373–1375. (2001).
- [10] Kempe, M., Stamm, U., Wilhelmi, B., and Rudolph, W., Spatial and temporal transformation of femtosecond laser pulses by lens systems, *J. Opt. Soc.* 38, 1058–1064. (1999).
- [11] Matei, G.O, Gili, M.A., Spherical aberration in spatial and temporal transformation of femtosecond laser pulses by lenses and lens systems, *J. Opt. Soc. Am. B* 9, 1158–1165. (1992).
- [12] Fuchs, U., Zeintner, U.D., and Tunnermann, A., Ultrashort pulse propagation in complex optical systems, *Opt. Express* 13, 3852–3861. (2005).
- [13] Leonid, S., Ferrari, A., and Bertolotti, M, Diffraction of a time Gaussian-shaped pulsed plane wave from a slit, *Pure. Appl. Opt* 5, 349–353. (1996).
- [14] Moulton, P.f, Quant. Electron. Conf., Munich, Germany, June (1982).
- [15] Holzwarth, “Measuring the Frequency of Light using Femtosecond Laser Pulses” aus Stuttgart den 21. December (2000).
- [16] Rulliere, C, Femtosecond laser pulses: principles and Experiments, *Springer*, (1998).
- [17] Joanna, M, “Seutp of very advanced for phase and amplitude reconstruction of electric field (VAMPIRE)” Master Thesis submitted to the Faculty for the Natural Sciences and for Mathematics of the Rostock University Germany (2007).
- [18] Abdolah, M.K, “Manipulation and characterization of femtosecond laser pulses for cluster spectroscopy” vorgelegt von aus Teheran (Iran) July (2007).
- [19] Greg, T, Andy, R Margaret, M, Measurement of 10 fs Laser Pulses. 1077-260X, IEEE (1996).
- [20] Hofmann, A, Bestimmung des elektrischen Feldes ultrakurzer Laserpulse mit SPIDER, Teil 1: Theorie, Projektpraktikumsbericht, Physikalisches Institut, EP1, Universität Würzburg (2005).
- [21] Jong Kook K. Investigation of high nonlinearity glass fibers for potential

applications in ultrafast nonlinear fiber devices, Dissertation submitted to the Faculty of the Virginia (2005).

[22] Khelladi.M, Seddiki.O, and Bendimerad.T, Time-Frequency Decomposition of an Ultrashort Pulse: Wavelet Decomposition, *Radioengineering ISSN*, April (2008) Vol.17, pp.1210–2512, N1

[23] Meyer,Y, Jaffort, S., Riol,O, waveletanalysis, *edition Française de scientifique American* (1987)